Desalination and Water Treatment
www.deswater.com
doi: 10.1080/19443994.2013.868837

53 (2015) 2905–2914
March

Taylor & Francis
Taylor & Francis Group

Removal of fluoride from aqueous media by magnesium oxide-coated nanoparticles

N. Minju[a], K. Venkat Swaroop[b], K. Haribabu[b,*], V. Sivasubramanian[b], P. Senthil Kumar[c]

[a]*Department of Chemical Engineering, Government Engineering College, Kozhikode, Kerala 673005, India*
[b]*Department of Chemical Engineering, National Institute of Technology Calicut, Kozhikode, Kerala 673601, India*
Tel. +91 9495224777; email: haribhabu@nitc.ac.in
[c]*Department of Chemical Engineering, SSN College of Engineering, Chennai 603110, India*

Received 20 June 2013; Accepted 18 November 2013

ABSTRACT

In the present study, magnesium oxide (MgO)-coated magnetite (Fe_3O_4) nanoparticles have been synthesized for analyzing the fluoride scavenging potential via modification of sol–gel method. The characterization of the nanoadsorbent was done by means of scanning electron microscopy, energy dispersive analysis of x-rays, and dynamic light scattering analyses. Batch adsorption experiments were carried out by varying the parameters adsorbent dose (0.75–3 g/L), initial fluoride concentration (5.6–25 mg/L), and pH (5.0–7.0). The maximum removal of fluoride was estimated as 98.6% for an initial fluoride concentration of 13.6 mg/L at optimal conditions: pH 6.0, adsorbent dosage of 2 g/L, and contact time of 120 min. Results revealed that the adsorption was rapid and the fluoride affinity depends on the solution pH, adsorbent dosage, and contact time. The equilibrium was obtained in less than 180 min. The adsorption kinetic data were fitted well to the pseudo-second-order kinetic model. The adsorption equilibrium data were best fitted to the Langmuir isotherm model. Based on the results observed, it was identified that the prepared adsorbent posses adequate adsorption potential to remove the fluoride ions from the aqueous solution.

Keywords: Magnesium oxide; Fluoride; Magnetite nanoparticles; Adsorption; Isotherm; Kinetics

1. Introduction

Fluoride is an essential nonmetal required for bone and enamel growth in humans. The existence of fluoride compounds in drinking water prevents tooth decay and strengthens the bones. According to World Health Organization (WHO) norms, the upper limit of fluoride concentration in drinking water is 1.5 mg/L [1]. But an intake of excess amount of fluoride for long duration causes fluorosis, a disease which damages (i) tooth enamel and leads to tooth decay, (ii) slackening, bending, and softening of bones [2]. The intake of fluoride is mainly in the form of drinking water and this is a very serious issue worldwide. The UNICEF's position on water fluoridation states that more than 25 countries around the world are endemic to this

*Corresponding author.

disease and the main countries got affected are central and western parts of China, Mexico, India (15 out of 32 states are affected). Fluoride is also taken by inhaling airborne fluoride released by burning of fluoride ores and fluorine-laden coal. The reported values of fluoride in groundwater is between 1 ppm to more than 35 ppm and in India it is found to be 38.5 ppm in some places.

This fluoride can be removed by various means such as adsorption [3,4], flocculation, ion-exchange method, and reverse osmosis etc. [5]. Of all these flocculation is the major technique in towns and reverse osmosis in cities. But adsorption is one of the new techniques that can be used for effective removal of excess of fluoride and this adsorption can be carried out using different adsorbents [6]. The major adsorbents based on activated alumina [7], modified activated alumina [8], lanthanum- and zirconium-impregnated adsorbents [9,10] have the limitation that during adsorption the coated elements may undergo leaching and get dissolved in water which when consumed causes health diseases and hence the use of these adsorbents is not encouraged and in some countries these are banned. So far, aluminum has been reported to be a neurotoxin, lanthanum to be mutagenic, and zirconium imparts serious health effects [11]. Hence their usage in drinking water is not good.

During the past few years, iron-based novel sorbents with strong affinity toward fluoride have been developed [12–14]. The recent trend is to develop processes for water treatment with iron oxide nanoparticles as adsorbents. The main iron-based adsorbents include schwertmannite [15], granular ferric hydroxide (GFH) [16], iron bearing oxide mineral i.e. goethite (α-FeOOH) [17], synthetic siderite [18] etc. Studies have also been reported on fluoride adsorption on some iron composite materials such as Fe-Ti oxide, Fe-Al-Ce trimetal oxide [19], Al/Fe-doped adsorbents [20], hydrous aluminium oxide embedded in Fe_3O_4 nanoparticles (Fe_3O_4@Al $(OH)_3$ NPs), and polypyrrole (PPy)/Fe_3O_4 magnetic nanocomposites. Magnetic nanosized adsorbents overcome the shortcoming of nonmagnetic nanomaterials and are very promising for preconcentration and removal of pollutants from environmental samples. Studies have reported that defluoridation using MgO could be an effective alternative for Nalgonda technique and activated alumina-based adsorption, which have been traditionally used in India for defluoridation process [21]. It is known that higher surface area and increased adsorption capacities for different contaminants is possible when the MgO crystal size is in the nanometer scale and smaller the crystallite size, better is the adsorption efficiency [22]. The adsorbent offers several advantages because of its large surface area and the nontoxic nature of magnesium [23,24]. Also, the magnetic property offers a way to use this adsorbent for the rapid treatment of large volumes of water with the help of an external magnetic field. Magnesium oxide is an important material for various applications including catalysis, waste remediation, and additives in refractory and paints and in particular has shown great promising application as a destructive adsorbent for toxic chemical agent [25].

In the present work, the nanoadsorbent such as MgO-coated Fe_3O_4 was successfully synthesized and it was performed as an adsorbent for water defluoridation process to test its effectiveness. The effect of operating parameters such as solution pH, adsorbent dose, initial fluoride ions concentration, and contact time on the removal of fluoride ions were carried out in a batch mode of operations. The equilibrium data were applied to the different adsorption isotherm models such as Langmuir and Freundlich adsorption isotherm models to get the relationship between the adsorbate in the liquid and solid phase at an equilibrium condition. The adsorption kinetic data were applied to the pseudo-first-order and pseudo-second-order kinetic models.

2. Experimental

2.1. Chemicals and materials

Pure Iron(II, III) oxide (Fe_3O_4)<50 nm particle size was purchased from Sigma-Aldrich, USA. Magnesium methoxide (Mg $(OCH_3)_2$), 7–8% in methanol was obtained from Alfa Aesar, India. Ethanol absolute (E. Merck, India) was purchased from Chemind Chemicals, Kozhikode. The pH of the solutions was adjusted by using the 0.1 M NaOH or 0.1 M HCl and the chemicals were procured from E. Merck, India. De-mineralized water brought from Nice Chemicals, Kannur was used. Sodium fluoride, NaF (E. Merck, India) was used for the preparation of the standard fluoride (100 mg/L) stock solution.

2.2. Preparation of MgO-coated Fe_3O_4 nanoparticles

The nanoparticles were prepared by proper modification of sol–gel procedure [26]. Initially, pure iron oxide nanoparticles about 6 grams was suspended in 1,000 mL ethanol. To this, a solution of 158.98 mL of magnesium methoxide in 3179.63 mL of distilled water was added. Then, the solution was thoroughly mixed and subjected to sonication for 60 min. If the

temperature increases when kept under sonication the water should be changed for every 15 min. Thus, sonicated solution is stirred for 12 h continuously at a speed of 750–800 rpm. After stirring, the solution was kept under simultaneous heating and stirring at 70˚C and 500 rpm, respectively, for about 5 h. Thus, prepared sample was centrifuged using cooling centrifuge (Rota-4R-V/F_M, India) for 10 min at 5,000 rpm. The residue thus obtained was washed with ethanol for two times and then heated at 600˚C in a muffle furnace (ROTEK, India) for drying for 15 min, then crushed, reheated for another 15 min and the procedure was repeated for several times until nano-sized particles were obtained.

2.3. Instruments

The microstructure and surface morphology of the synthesized nanoadsorbent were studied using Scanning Electron Microscope (SEM) (Hitachi, Model SU6600). The accelerating voltage applied was 15 kV. The specimens were coated with 50 μm of thick gold film in an automatic sputter coater to avoid charging under an electron beam prior to SEM studies. Characterization of the sample was carried out at three magnifications of 9,000, 30,000, and 70,000. The elemental analysis for oxygen, magnesium, and iron were carried out with Energy Dispersive Analysis of X-rays (EDAX). The zeta potential and size distribution of the sample were performed with a Zetasizer Ver. 6.20 (Malvern Instruments Ltd., UK). The pH measurements were performed with a digital pH meter.

2.4. Fluoride analysis and batch fluoride adsorption experiments

For the removal of fluoride, a solution of 100 mg/L was prepared (stock solution) by dissolving 0.221 g of NaF in 1 L of deionized water. All the solutions for fluoride removal experiments and analysis were prepared by appropriate dilutions of this stock solution. Studies were done by varying the parameters such as adsorbent dosage, initial concentration, and pH of the solution. The solutions for the experiment were prepared by taking 100 mL of F^- containing solution in a 250 mL conical flask with the required amount of adsorbent (0.075–0.2 g) and shaking in a mechanical incubator/shaker (ROTEK, India) with vigorous stirring at 300 rpm for varying contact time. All the experiments were carried out at 28 ± 1˚C since all practical applications rely up on room temperature. The rapid separation of the nanoparticles after defluoridation procedure was made possible by a strong magnet (rectangular shape, 40 × 40× 20 mm). Then, the magnet was placed at the bottom of the conical flask and appropriate settling time was allowed after which 2 mL of the sample was withdrawn and analyzed for residual F^- content using HI 96739 Ion Selective Meter from HANNA Instruments, Europe equipped with the accessories HI 93739A-0 fluoride high range reagent A and HI 93739B-0 fluoride high range reagent B.

2.5. Adsorption isotherm studies

Adsorption isotherm studies were conducted with initial concentrations ranging from 0 to 25 mg/L using batch procedure at 28 ± 1˚C in deionized water at a pH 6.0 and 2 g/L adsorbent dose in 250 mL conical flasks. The adsorbed amount of F^- ion per unit mass of MgO-coated Fe_3O_4 nanoparticles at an equilibrium time, q_e (mg/g), was calculated from the mass balance equation as:

$$q_e = \frac{(C_i - C_e)V}{m} \tag{1}$$

where C_i and C_e (mg/L) are the initial F^- ion concentration and F^- ion concentration at equilibrium, respectively; V is the volume of F^- ion solution (L); and m is the mass of adsorbent (g). The removal efficiency of adsorbent on F^- ion was measured as follows:

$$\%\ \text{Removal} = \frac{C_i - C_f}{C_i} \times 100 \tag{2}$$

where C_i and C_f are the initial and final equilibrium concentration of F^- ion (mg/L) in aqueous solution, respectively.

2.6. Adsorption kinetic studies

Kinetic studies were performed at room temperature with 200 mg of adsorbent in 100 mL fluoride solutions with fixed initial concentrations 12, 16.1, and 19.8 mg/L by agitation at 300 rpm in an incubator/shaker at optimum pH. The time interval is fixed from 30 to 270 min at which 2 mL of sample is withdrawn every 30 min and the residual fluoride content is analyzed. The amount of fluoride ions adsorbed onto the adsorbent at time t, q_t (mg/g), was calculated by the following equation:

$$q_t = \frac{(C_i - C_t)V}{m} \tag{3}$$

where C_t is the concentration of F^- ion in the solution at time t (mg/L).

3. Results and discussion

3.1. Characterization of MgO coated Fe_3O_4 nanoparticles

The SEM micrograph contains information about the samples surface topology and composition. SEM images of the prepared MgO-coated Fe_3O_4 nanoparticles observed under high vacuum and suspended in ethanol are shown in Fig. 1. The images of the synthesized samples reveal the particle size and a highly porous structure under vacuum (Fig. 1(a)). As can be seen from Fig. 1(b), under wet conditions, the micrograph shows small individual spherical particles without any agglomeration of which most having sizes below 100 nm. This is mainly due to the nanosize of Fe_3O_4, which is <50 nm. The core–shell-structured nanoparticles have an average size of 98.3 nm (Fig. 1(c)). The EDAX spectrum of the MgO-coated Fe_3O_4 nanoparticles are shown in Fig. 2. It confirms the presence of elements magnesium, oxygen, and iron. The DLS method was used to find out zeta potential and hydrodynamic diameter of sample. The significance of zeta potential is that its value can be related to the stability of dispersed solutions. For molecules and particles that are small enough, a high zeta potential will confer stability, i.e. the solution or dispersion will resist aggregation. When the potential is low, attraction exceeds repulsion and the dispersion will break and flocculate. So, colloids with high zeta potential (negative or positive) are electrically stabilized, while colloids with low zeta potentials tend to coagulate or flocculate [27]. From the zeta potential curve (Fig. 3(a)) of the sample it is seen that the first peak occurs at 16 mV. In the range of 16–45 mV, the total count is maintained as ~830,000. A zeta potential in this range shows the good stability of the solution. The particle size distribution curve of the sample is shown in Fig. 3(b). It indicated that the particle size is in the range 100–400 nm and the average particle size is about 355.7 nm.

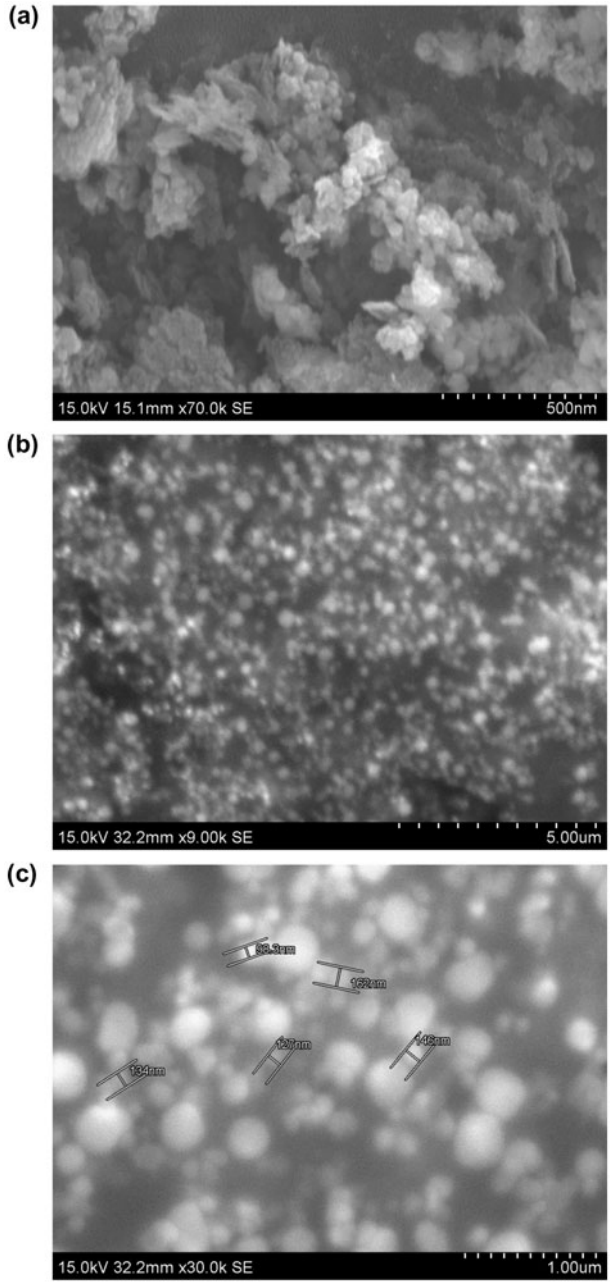

Fig. 1. SEM micrographs of synthesized MgO coated Fe_3O_4 under vaccum (a); suspended in ethanol (b–c).

3.2. Batch adsorption experiments

3.2.1. Effect of adsorbent dose

A significant increase in adsorption occurs with the increase in dosage from 0.75 to 3 g/L as seen in Fig. 4. This may be due to the increased availability of binding sites with increase in adsorbent dosage. Maximum adsorption occurs with 2 g/L of adsorbent dose and afterward. Nearly 98% of the fluoride was removed using 2.5 g/L of adsorbent. After a dosage of 2.5 g/L the ratio of fluoride ions available to the nanoadsorbent dose is very negligible which further results in a constant removal efficiency.

3.2.2. Effect of initial concentration

As fluoride ion concentration changes from place to place, different fluoride ion concentrations have

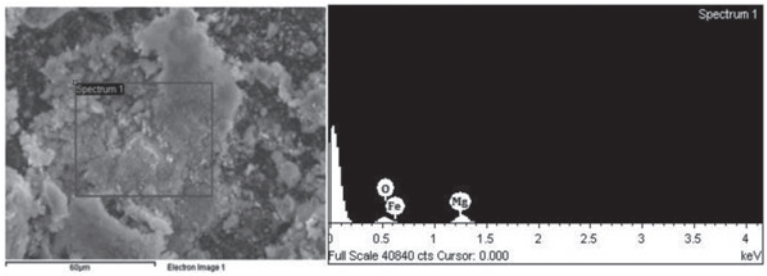

Element	Weight %	Atomic %
O K	36.61	55.54
Mg K	30.02	29.96
Fe K	33.37	14.50
Totals	100.00	

Fig. 2. EDAX spectrum and elemental composition of the synthesized MgO coated Fe_3O_4 nanoparticles.

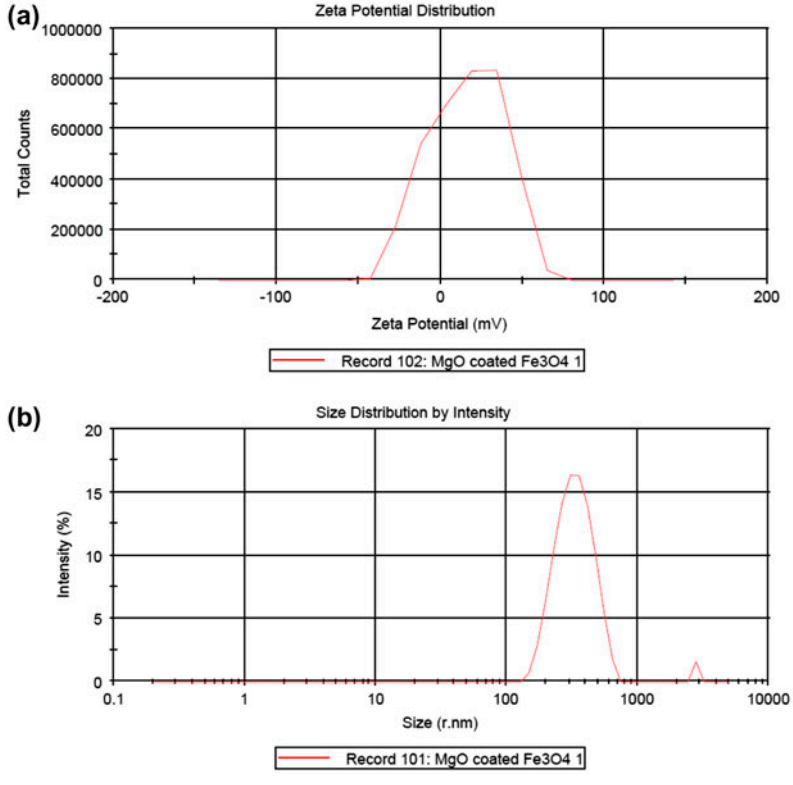

Fig. 3. Distribution curves for zeta potential (a); particle size (b).

been taken and adsorption experiments were done in order to find the effectiveness of the adsorbent. For this purpose, adsorbent dosage of 2 g/L in every sample with varying initial concentrations were kept under shaking at 300 rpm speed and room temperature at neutral pH. The samples were analyzed for every 30 min. and the percentage removal was calculated. The concentration of the sample is uniform

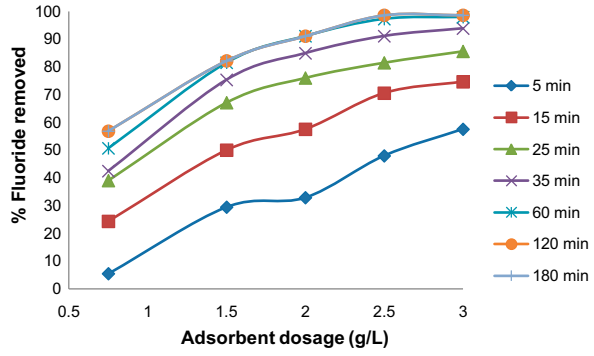

Fig. 4. Effect of adsorbent dose on F^- removal. Conditions: initial concentration 14.6 mg/L, pH 7.0, temperature 28 ± 1°C, contact time 5–180 min.

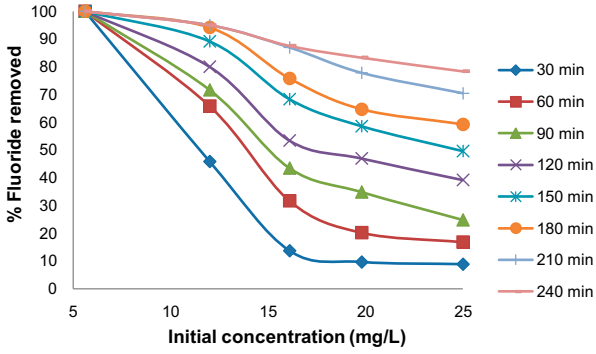

Fig. 5. Effect of initial concentration on F^- removal. Conditions: adsorbent dose 2 g/L, pH 7.0, temperature 28 ± 1°C, contact time 30–240 min.

throughout and since all the adsorbent particles are completely settled at the bottom during the withdrawal of sample for analysis no change in adsorbent dose is observed; thus mass of the system is conserved. The values are plotted in Fig. 5. Adsorbent works excellently for low- and medium-concentrated samples and good for high concentrations. As the fluoride concentration increases the adsorbed amount of fluoride also increases. For sample, with 5.6 mg/L initial concentration 100% removal efficiency is obtained. Here, the ratio of surface active sites to fluoride ions is high. This reveals the good possibility of adsorbent for use in drinking water samples. The effectiveness of the sample decreases drastically for concentrations greater than 20 mg/L which may be due to the increase in presence of fluoride ions leading to saturation of active sites on the adsorbent surface.

3.2.3. Effect of solution pH

The literature studies reveal that the adsorption was influenced by pH in the range 5.0–7.0 (Table 1). Hence, effect of solution pH was studied for pH varying from 5.0 to 7.0 and values are plotted in Fig. 6. In the region of pH 5, there may be formation of HF which reduces the availability of F^- ions thus decreasing the removal efficiency. The F^- removal reaches 98.5% at pH 6.0 which is considered as optimum value. Afterward, the percentage removal starts decreasing indicating the upcoming effect of hydroxyl ions. Since the groundwater pH is in the range of 6.0–8.0, the present nanoadsorbent can be effectively applied for F^- removal.

3.3. Adsorption kinetics

The adsorption kinetic data are analyzed according to the two different kinetic models such as pseudo-first-order and pseudo-second-order kinetic models. The mathematical representations of the two models are described by the following equations.

Table 1
Comparison of loading capacities of various adsorbents for fluoride

Adsorbent	pH	Initial F^-	Temp.	Contact time	Adsorption capacity	Refs.
MASG	6.0	–	298 K	–	38 g/kg	[6]
MAHP					8 g/kg	
GZI	7.0	10 mg/L	25°C	10 h	9.80 mg/g	[10]
Mg-HAp	6.5	1.5–13 mg/L	30 ± 2°C	24 h	6.211 mg/g	[11]
Iron (III)-tin(IV) mixed oxide	6.4 ± 0.2	10–50 mg/L	30 ± 1.6°C	2 h	10.47 mg/g	[13]
Fe_3O_4@Al(OH)$_3$	6.5	0–160 mg/L	25°C	240 min	88.48 mg/g	[14]
GFH	6.0–7.0	1−100 mg/L	25°C	24 h	7.0 mg/g	[16]
Synthetic nano hydroxyapatite	5.0–6.0	3–80 mg/L	298 K	100 min	4.575 mg/g	[29]
Al_2O_3/CNTs	6.0	50 mg/L	25°C	12 h	28.7 mg/g	[30]
nano-AlOOH	5.2 ± 0.2	3–35 mg/L	298 K	6 h	3,259 mg/kg	[31]
Fe-Al-Ce nano adsorbent	7.0	0.001 M	25°C	36 h	2.22 mg/g	[32]
MgO coated Fe_3O_4	6.0	13.6 mg/L	28 ± 1°C	2.5 h	10.96 mg/g	Present study

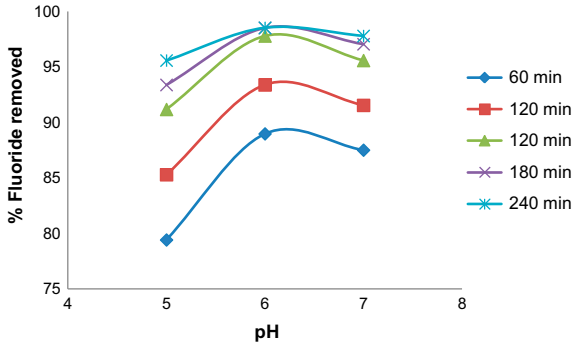

Fig. 6. Effect of solution pH on F^- removal. Conditions: adsorbent dose 2 g/L, initial concentration 13.6 mg/L, temperature 28 ± 1°C, contact time 60–240 min.

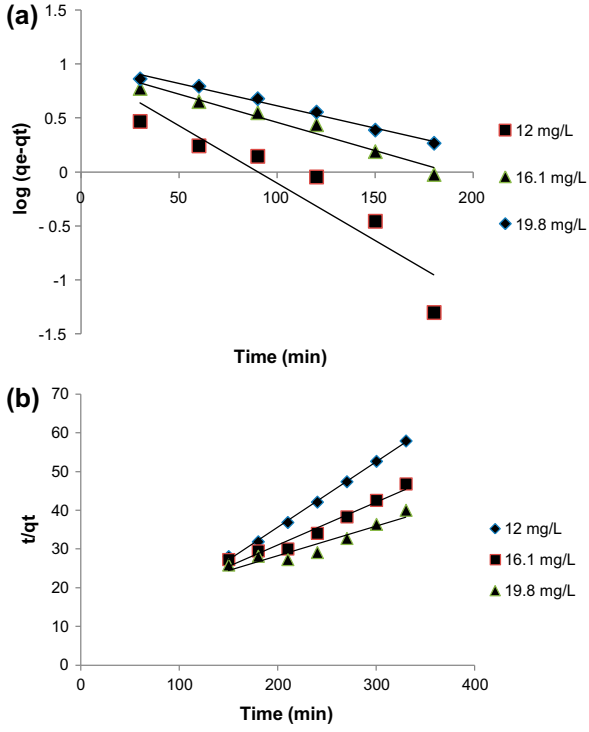

Fig. 7. Kinetic plots: (a) pseudo-first order; and (b) pseudo-second order.

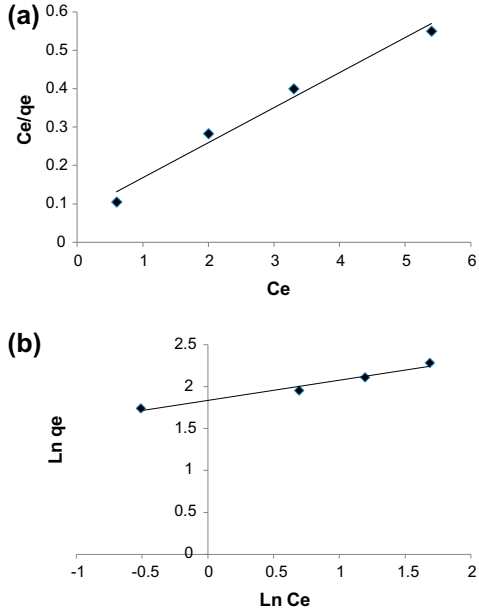

Fig. 8. (a) Langmuir isotherm plot; and (b) Freundlich isotherm plot.

Pseudo-first-order kinetic model is given as follows:

$$\log(q_e - q_t) = \log q_e - \frac{k_1}{2.303}t \tag{4}$$

and pseudo-second-order kinetic equation is given as follows:

$$\frac{t}{q_t} = \frac{1}{k_2 q_e^2} + \frac{1}{q_e}t \tag{5}$$

where q_e and q_t are the amount of fluoride adsorbed per unit mass of adsorbent at equilibrium and at any time t (mg/g), respectively. k_1 and k_2 are the rate constants for pseudo-first-order and pseudo-second-order sorption in (1/min) and (g/mg/min), respectively. The kinetic results are shown in Fig. 7. The rapidity in

Table 2
Kinetic parameters for F^- adsorption on MgO coated Fe_3O_4

Initial concentration (mg/L)	q_e experimental (mg/g)	Pseudo-first order			Pseudo-second order		
		k_1 (1/min)	q_e (mg/g)	r^2	q_e (mg/g)	k_2 (mg/gmin$^{(1/2)}$)	r^2
12	5.7	0.02441	9.036	0.8626	5.677	−5,291	0.9961
16.1	7.05	0.01202	9.527	0.9654	6.863	−2,822	0.8589
19.8	8.25	0.00948	10.568	0.9865	7.847	−2,139	0.9011

Table 3
Langmuir and Freundlich isotherm for F^- adsorption on MgO coated Fe_3O_4

	Isotherm models					
	Langmuir model			Freundlich model		
Parameters	q_e (mg/g)	b (L/mg)	r^2	K_F ($mg^{1-(1/n)}L^{(1/n)}g^{-1}$)	n	r^2
MgO-coated Fe_3O_4	10.96	1.188	0.9799	6.2776	4.15	0.9688

the uptake kinetics can be explained in terms of reduction in diffusion path and increase in exposed surface area. As material tends toward nano-scale size, the distance an adsorbing species travels to reach the active sites is significantly reduced, the external surface area per unit mass is increased and hence the adsorbing species experiences reduced diffusion resistance leading to faster kinetics [28]. The correlation coefficients and kinetic parameters for the two models were calculated from the plots of log ($q_e - q_t$) vs. t and (t/q_t) vs. t, respectively. The r^2 values and the kinetic parameters are tabulated in Table 2. Though the r^2 values for first-order plots were >0.85, there is large deviation in the experimental and calculated q_e values which infers that the kinetics is well predicted by pseudo-second-order model with regression coefficients of 0.9961, 0.8589, and 0.9011, respectively, for 12, 16.1, and 19.8 mg/L initial concentration. The q_e values obtained are 5.677, 6.863, and 7.847 which is almost similar to the experimental q_e values 5.7, 7.05, and 8.25 mg/g, respectively.

3.4. Adsorption equilibrium

In any batch adsorption system, the adsorption capacity is one of the basic parameters used for design of the system. Equilibrium studies are conducted to determine the condition at which maximum amount of fluoride is removed using the synthesized nanoadsorbent. From the experimental studies conducted, it is observed that the adsorption capacity reaches a certain equilibrium value beyond which no change is observed in the residual fluoride concentration. The equilibrium studies are conducted at room temperature (28 ± 1°C) with varying initial concentrations at pH 6.0. The adsorption process can be expressed with the help of either of the two models Langmuir or Freundlich. The Langmuir adsorption equation relates the coverage or adsorption of molecules on a solid surface to concentration of a medium above the solid surface at a fixed temperature. The equation was developed by Irving Langmuir in 1916. The Langmuir equation is valid for monolayer sorption onto a surface with a finite number of identical sites and is given as:

$$q_e = \frac{q_m K_L C_e}{1 + K_L C_e} \tag{6}$$

Rewriting:

$$\frac{1}{q_e} = \frac{1}{q_m} + \frac{1}{q_m K_L}\frac{1}{C_e} \tag{7}$$

where q_m and K_L are the Langmuir constants, q_e is the amount adsorbed at equilibrium (mg/g), and C_e is the equilibrium concentration (mg/L). The slope and intercept of the equation is determined by plotting ($1/q_e$) vs. ($1/C_e$).

Freundlich adsorption isotherm is a curve relating the concentration of a solute on the surface of an adsorbent to the concentration of the solute in the liquid with which it is in contact. It was proposed by Freundlich in 1909. Here, the amount of mass that is adsorbed is plotted against temperature which gives the variation of adsorption with temperature. It is an indicative of the surface heterogeneity of the sorbent, given by the equation:

$$q_e = K_F C_e^{1/n} \tag{8}$$

Rewriting:

$$\log q_e = \log K_f + \frac{1}{n}\log C_e \tag{9}$$

where K_f and n are the Freundlich constants which indicate the adsorption capacity and adsorption intensity. The slope and intercept are given by K_f and n.

The adsorption results are shown in Fig. 8. The data points fitted very well to the Langmuir model with a regression coefficient of about 0.9799. The parameters for both the models are tabulated in Table 3. The Langmuir constant "b" is 1.188 L/mg which indicates good heat of adsorption. The loading

capacity of 10.96 mg/g is compared with the values reported in the literature (Table 1). Since fluoride is highly electronegative and has high bond strength, a higher "*n*" value is obtained which indicates the bond strength between adsorbate and adsorbent.

4. Conclusions

Magnesium oxide coated magnetite nanoparticles were synthesized by proper modification of sol–gel method. The adsorbent showed an excellent fluoride scavenging potential for concentrations below 10 mg/L which makes them a potential candidate for drinking water defluoridation process. Under optimal conditions (adsorbent dose: 2 g/L, pH 6.0, contact time: 120 min) for an initial concentration of 13.6 mg/L, the percentage removal efficiency was 98.5%. The Langmuir monolayer adsorption capacity was found to be 10.96 mg/g. The kinetic data followed pseudo-second-order model.

Acknowledgment

The authors are thankful to Mr. Balamurugan, Research Scholar, School of Nanoscience and Technology, NIT Calicut for his help in interpreting the SEM micrographs.

References

[1] World Health Organization (WHO), Guidelines for Drinking-Water Quality: Incorporating First Addendum Recommendations, 3rd ed, 1 (2006) 375–376.
[2] A. Bhatnagar, E. Kumar, M. Sillanpaa, Fluoride removal from water by adsorption—A review, Chem. Eng. J. 171 (2011) 811–840.
[3] M. Mohapatra, S. Anand, B.K. Mishra, D.E. Giles, P. Singh, Review of fluoride removal from drinking water, J. Environ. Manage. 91 (2009) 67–77.
[4] X.P. Liao, B. Shi, Adsorption of fluoride on zirconium (IV) – Impregnated collagen fiber, Environ. Sci. Technol. 39 (2005) 4628–4632.
[5] J.J. Schoeman, A. Steyn, Defluoridation, denitrification and desalination of water using ion-exchange and reverse osmosis, WRC Report No 124/00, Water Research Commission, Pretoria, 2000.
[6] C.-F. Chang, P.-H. Lin, W. Holl, Aluminium-type superparamagnetic adsorbents: Synthesis and application on fluoride removal, Colloids Surf. 280 (2006) 194–202.
[7] H. Farrah, J. Slavek, W.F. Pickering, Fluoride interactions with hydrous aluminium oxides and alumina, Aust. J. Soil Res. 25 (1987) 55–69.
[8] S.A. Wasay, S. Tokunaga, S.W. Park, Removal of hazardous anions from aqueous solutions by La (III) - and Y (III) impregnated alumina, Sep. Sci. Technol. 31 (1996) 1501–1514.
[9] T. Poursaberi, M. Hassanisadi, K. Torkestani, M. Zare, Development of zirconium (IV)-metalloporphyrin grafted Fe_3O_4 nanoparticles for efficient fluoride removal, Chem. Eng. J. 189–190 (2012) 117–125.
[10] X. Dou, Y. Zhang, H. Wang, T. Wang, Y. Wang, Performance of granular zirconium-iron oxide in the removal of fluoride from drinking water, Water Res. 45 (2011) 3571–3578.
[11] P. Garg, S. Chaudhari, Adsorption of fluoride from drinking water on magnesium substituted hydroxyapatite, Int. Conf. Fut. Environ. Energ, 28 (2012) 180–185.
[12] L. Chen, B.-Y. He, S. He, T.-J. Wang, C.-L. Su, Y. Jin, Fe-Ti oxide nano-adsorbent synthesized by co-precipitation for fluoride removal from drinking water and its adsorption mechanism, Powder Technol. 227 (2012) 3–8.
[13] K. Biswas, K. Gupta, U.C. Ghosh, Adsorption of fluoride by hydrous iron(III)- tin(IV) bimetal mixed oxide from the aqueous solutions, Chem. Eng. J. 149 (2009) 196–206.
[14] X. Zhao, J. Wang, F. Wu, T. Wang, Y. Cai, Y. Shi, G. Jiang, Removal of fluoride from aqueous media by Fe_3O_4@$Al(OH)_3$ magnetic nanoparticles, J. Hazard. Mater. 173 (2010) 102–109.
[15] A. Eskandarpour, M.S. Onyango, A. Ochieng, S. Asai, Removal of fluoride ions from aqueous solution al low pH using schwertmannite, J. Hazard. Mater. 152 (2008) 571–579.
[16] E. Kumar, A. Bhatnagar, M. Ji, W. Jung, S.-H. Lee, S.-J. Kim, G. Lee, H. Song, J.-Y. Choi, J.-S. Yang, B.-H. Jeon, Defluoridation from aqueous solutions by granular ferric hydroxide (GFH), Water Res. 43 (2009) 490–498.
[17] M. Mohapatra, K. Rout, S.K. Gupta, P. Singh, S. Anand, B.K. Mishra, Facile synthesis of additive-assisted nano goethite powder and its application for fluoride remediation, J. Nanopart. Res. 12 (2010) 681–686.
[18] Q. Liu, H. Guo, Y. Shan, Adsorption of fluoride on synthetic siderite from aqueous solution, J. Fluorine Chem. 131 (2010) 635–641.
[19] X. Wu, Y. Zhang, X. Dou, M. Yang, Fluoride removal performance of a novel Fe-Al-Ce trimetal oxide adsorbent, Chemosphere 69 (2007) 1758–1764.
[20] V. Kumar, N. Talreja, D. Deva, N. Sankararamakrishnan, A. Sharma, N. Verma, Development of bi-metal doped micro- and nano multi-functional polymeric adsorbents for the removal of fluoride and arsenic(V) from wastewater, Desalination 282 (2011) 27–38.
[21] S.M. Maliyekkal, K.R. Anshup, T. Antony Pradeep, High yield combustion synthesis of nanomagnesia and its application for fluoride removal, Sci. Total Environ. 408 (2010) 2273–2282.
[22] B. Nagappa, G.T. Chandrappa, Mesoporous nanocrystalline magnesium oxide for environmental remediation, Microporous Mesoporous Mater. 106 (2007) 212–218.
[23] V. Aravind, K.P. Elango, Adsorption of fluoride onto magnesia-equilibrium and thermodynamic study, Indian J. Chem. Technol. 13 (2006) 476–483.
[24] M. Mohapatra, D. Hariprasad, L. Mohapatra, S. Anand, B.K. Mishra, Mg-doped nanoferrihydrite—A new adsorbent for fluoride removal from aqueous solutions, Appl. Surf. Sci. 258 (2012) 4228–4236.

[25] Z.-X. Tang, L.-E. Shi, Preparation of nano-MgO using ultrasonic method and its characteristics, J. Ecl. Quím. Sao Paulo 33(1) (2008) 15–20.
[26] L.D. Matteis, L. Custardoy, R. F. Pacheco, C. Magen, J.M. Fuente, C. Marquina, M.R. Ibarra, Ultrathin MgO coating of superparamagnetic magnetite nanoparticles by combined coprecipitation and sol−gel synthesis, Chem. Mater 24 (2012) 451–456.
[27] D. Hanaor, M. Michelazzi, C. Leonelli, C.C. Sorrell, The effects of carboxylic acids on the aqueous dispersion and electrophoretic deposition of ZrO_2, J. Eur. Ceram. Soc 32 (2012) 235–244.
[28] M. Bhaumik, T.Y. Leswifi, A. Maity, V.V. Srinivasu, M.S. Onyango, Removal of fluoride from aqueous solution by polypyrrole/Fe_3O_4 magnetic nanocomposite, J. Hazard. Mater. 186 (2011) 150–159.
[29] S. Gao, J. Cui, Z. Wei, Study on the fluoride adsorption of various apatite materials in aqueous solution, J. Fluorine Chem. 130 (2009) 1035–1041.
[30] Y.-H. Li, S. Wang, A. Cao, D. Zhao, X. Zhang, C. Xu, Z. Luan, D. Ruan, J. Liang, D. Wu, B. Wei, Adsorption of fluoride from water by amorphous alumina supported on carbon nanotubes. Chem. Phys. Lett. 350 (2001) 412–416.
[31] S.-G. Wang, Y. Ma, Y.-J. Shi, W.-X. Gong, Defluoridation performance and mechanism of nano-scale aluminum oxide hydroxide in aqueous solution. J. Chem. Technol. Biotechnol. 84 (2009) 1043–1050.
[32] L. Chen, H.-X. Wu, T.-J. Wang, Y. Jin, Y. Zhang, X.-M. Dou, Granulation of Fe-Al-Ce nano-adsorbent for fluoride removal from drinking water by spray coating on sand in a fluidized bed, Powder Technol. 193 (2009) 59–64.